Title

Numerical modeling of scattering from discrete fracture zones in a San Juan Basin gas reservoir

Permalink

https://escholarship.org/uc/item/1gt1k6f5

Authors

Daley, T.M.
Nihei, K.T.
Myer, L.R.
et al.

Publication Date

2002-08-01

Numerical modeling of scattering from discrete fracture zones in a San Juan Basin gas reservoir

T.M. Daley, K.T. Nihei, L.R. Myer, E.L. Majer, Lawrence Berkeley National Laboratory, J.H. Queen, M. Fortuna, J. Murphy, Conoco, Inc, R.T. Coates, Schlumberger-Doll Research.

Summary

Numerical modeling of the seismic response to discrete fracture zones has been conducted to aid gas exploration in the San Juan Basin. A 2D, anisotropic, finite-difference code was used with vertical fracture zones represented by a single column of anisotropic grid points. Scattering, including strong P-to-S mode conversions was observed using surface seismic acquisition geometry. Fractures (or joints) were represented by their stiffness. Since field scale stiffness measurements are lacking, we used a fracture stiffness value derived from lab studies and a conceptual model. Two scales of fracturing were investigated using a basic 5-layer model. Observable scattering was demonstrated in a more realistic 45-layer model. The moveout of the fracture generated events on common mid-point (CMP) gathers is such that standard processing would treat this energy as "noise". Observation of coherent scattered events implies that direct imaging of gas-filled fracture zones is possible.

Introduction

As part of a Dept. of Energy sponsored program in fractured gas production, we are conducting numerical modeling of seismic wave propagation in fractured media (Majer, et al., 2001, Majer, et al., 2002). We are using the San Juan Basin in Northwest New Mexico as a focus area and investigating the seismic detection of fracturing which may control gas production. 3D surface seismic data, acquired and reprocessed by Conoco, is being analyzed for fracture-induced effects beginning with equivalent anisotropic media based P-wave analysis. Our numerical modeling is focused on a different approach. We are studying the seismic effects of discrete fractures (or fractures zones) set in an isotropic background rather than using equivalent anisotropic media approximations. Numerical modeling of discrete fractures will be used to guide future acquisition and analysis of surface and borehole seismic data with the goal of imaging discrete gas-filled fracture zones.

Theory and Method

The finite-difference code uses a standard 2D staggered-grid, velocity-stress, anisotropic algorithm. The fractures are modeled as finite length columns of single grid points with equal normal and tangential stiffness (representing gas-filled fractures or joints). For a given fracture stiffness in a given background, the anisotropic elastic constants are defined and the wavefield is modeled using the method of Coates and Schoenberg (1995). The F-D solution was tested against boundary element methods (Nihei, et al. 2001) and two independent F-D implementations.

An important component of this work is developing an understanding of field scale fracture properties. Before beginning modeling, fracture stiffness needs to be assigned. In-situ values of fracture stiffness could not be obtained and, in general, there is a poor understanding of what the value should be for fractures in a gas reservoir. For an idealized model of two rough surfaces in contact with constant void size and spacing, stiffness can be analytically determined as shown in Figure 1. Laboratory studies show that contact area increases as stress increases, but even at stresses representative of reservoir conditions, contact areas may be less than 40%. Calculations were carried out for a range in values of contact area and void size, resulting in the selection of a stiffness value of $8x10^9$ Pa/m for the short, stiff fractures in our basic model (Figure 2). The longer, more compliant fracture zones (joints) were arbitrarily assigned a stiffness 1/10 of the stiff fractures ($8x10^8$ Pa/m).

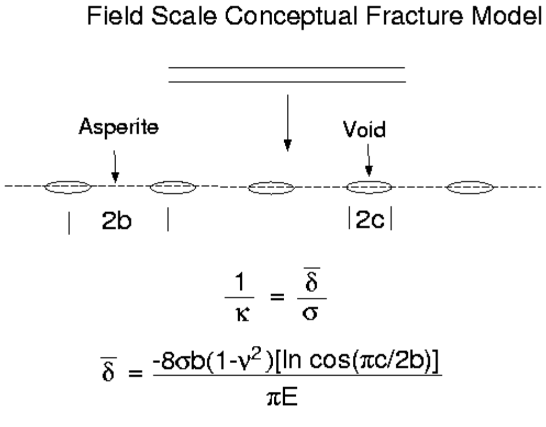

$$\frac{1}{\kappa} = \frac{\bar{\delta}}{\sigma}$$

$$\bar{\delta} = \frac{-8\sigma b(1-\nu^2)[\ln\cos(\pi c/2b)]}{\pi E}$$

Figure 1. The calculation of fracture stiffness used in F-D modeling begins with estimates of constant contact area, (e.g. 30%, where 1-c/b = 0.3) and void length (e.g. 0.25 m). Assuming a constant far-field applied stress (σ), the fracture stiffness (κ), associated with additional

displacement (δ) is calculated from the crack geometry (void spacing and length, b and c), along with the Young's modulus (E) and Poisson's ratio (ν) of the host material. For constant contact area of 30% (1-c/b = 0.3) and void length c = 0.25 m, then k = 9×10^9 Pa/m.

Basic Model (5 Layers, 2 Fracture Sets)

To study the fracture effects on surface seismic data at field scales, a 5-layer model was developed based on the Mesa Verde Unit of the San Juan Basin. Two scales of fracturing were investigated using the assumption that the fracturing was bed-terminated and had horizontal spacing approximately equal to vertical length. Long, compliant joints spanned the Mesa Verde unit while short, stiff fractures spanned the Cliffhouse sandstone member. Specifically, 4 through-going, compliant joints were 650 m long with 600 m spacing, and 107 bed-truncated stiff fractures were 60 m long with 21 m spacing. The entire model has 1050 x 1050 grid points at 3 m spacing (with a 150 grid point absorbing boundary is on all sides) giving a useable 2250 x 2250 m model. Shot gathers were generated using a point source with a 50 Hz Ricker wavelet and 38 sensors at 60 m spacing.

A wavefield snapshot of the horizontal component of velocity is shown in Figure 3. Note the strong scattering and complex wavefield. Among the observed events are strong P-to-S conversions and fracture-tip diffractions. The fracture tip diffractions may not be realistic for field scale joints because the joints may not have sharply truncated tips. The P-to-S conversions ("V" shapes in Figure 3) should be observable. Because the converted energy is downgoing, VSP geometry should give the best opportunity for field observation, however, surface observations will include upgoing fracture scattered events which have been reflected from the velocity interfaces

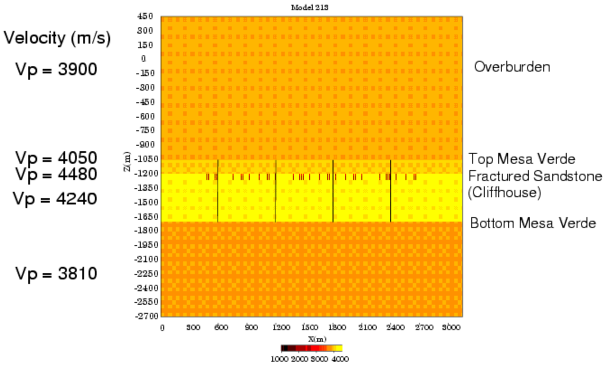

Figure 2 A five layer, 2 fracture set model of the San Juan Basin with focus on the Mesa Verde Unit

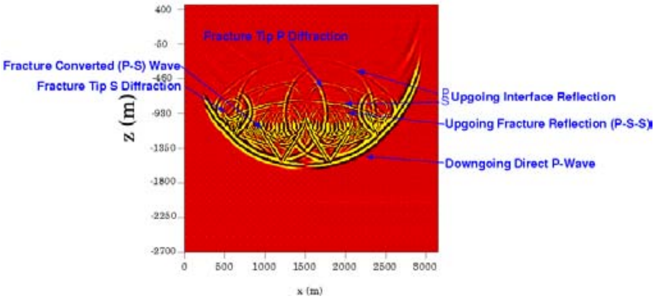

Figure 3 Wavefield snapshot at 400 ms time in the 5-layer model. The horizontal component of motion is plotted.

The effect of fracture scattering on surface seismic observations is shown in Figure 4 which compares a shot gather for the same model with and without the fracture sets. Traces are the vertical component at true relative amplitude. Many coherent events are generated by the discrete fractures. Note that most of the fracture scattered energy is following the reflection for the interface below the fractures (the base of the Mesa Verde at about 800 ms).

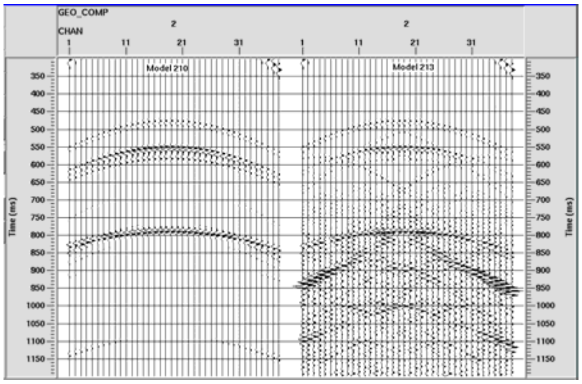

Figure 4 Comparison of the basic model shot gather with no fractures (left) and both fracture sets (right). Data is vertical component at true relative amplitude.

Having demonstrated that scattering from discrete fracture zones could be observed with a surface seismic geometry, various studies were conducted using shot gathers. Comparing shot gathers with large fractures (joints) only to the one with both fracture sets, we see that the dominant energy is scattered from the 4 discrete fractures with lower stiffness. A modeled shot only the 107 thin-layer fractures shows that instead of the coherent events seen from the large fractures, "ringing" arrivals from multiple scattering are observed. Calculation of divergence and curl of the numerical data allows us to separate P and S energy. This study showed both P-P and P-S scattering is observable. We added attenuation to various model elements including the overburden (Q=50), the thin layer (Q=40) and the fractures themselves (Q=25). All these cases still contain significant energy scattered from fractures. An important result is the range of fracture stiffness values which may be detectable via scattering in field data (allowing for a "noise free" model). This range is within the values derived from our conceptual model (10^8 to 10^9 Pa/m).

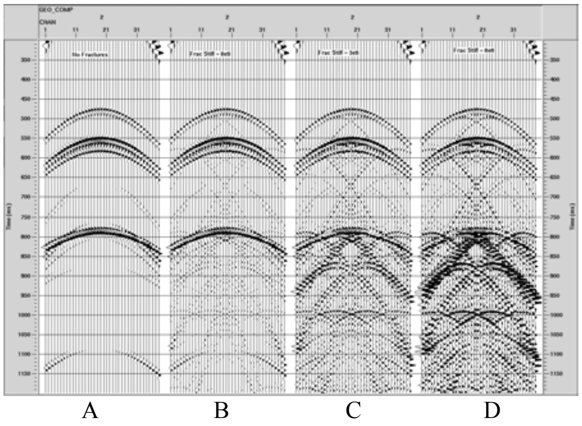

Figure 5 Shot gathers of vertical component over the basic model with only large fractures and decreasing stiffness:
A) No fractures (infinite stiffness);
B) Fracture stiffness = $8x10^9$;
C) Fractures stiffness = $3x10^9$;
D) Fracture stiffness = $8x10^8$.
All traces are true relative amplitude

Realistic Model (45 Layers, 1 Fracture Cluster) with CMP Data

In order to study a more "realistic" velocity structure for the basin, a 6x3 km. 45 layer model was developed based on blocked well logs from the basin. One fracture "cluster" with a long, central, compliant fracture and shorter, stiffer fractures on either side was placed in the Mesa Verde Unit. Figure 6 shows the scattering in a vertical component shot gather. The horizontal component (not shown) also has significant fracture scattered energy.

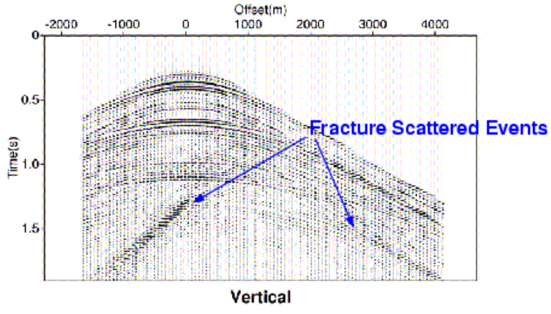

Figure 6 Vertical component shot gather for the 45-layer model. Note that events with non-hyperbolic moveout are fracture scattered events. These fracture scattered events can still be detected within the complex reflectivity of a 45 layer model.

In order to investigate the effects of discrete fracture scattering in a CMP section, over one hundred shot gathers were computed, sorted into CMP gathers and corrected for normal moveout (NMO). In this NMO corrected data, shown in Figure 7, horizontal events are the velocity interfaces, while dipping events cross-cutting interface reflections are fracture scattered events. In "standard" processing, the fracture scattered events would be intentionally removed or attenuated to "improve" the CMP stack.

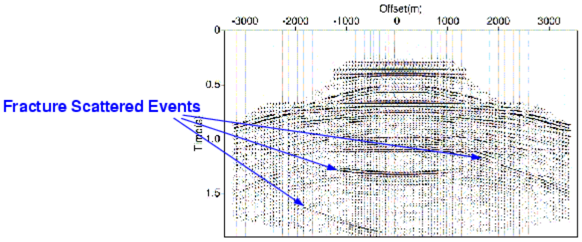

Fracture Scattered Events

Figure 7 NMO corrected CMP gather for a 45 layer model with one fracture cluster.

Because of the strong P-to-S conversions observed in the modeling, a divergence-curl imaging method was tested. The approach is an adaptation of reverse-time migration. The wavefield recorded at the receiver array is used for back propagation of the scattered curl wavefield. Concurrently, the divergence wavefield from the source is forward propagated into the medium. An image of the scatterers is formed by multiplying source-divergence and receiver-curl wavefields at each time step and adding images obtained at earlier time steps to form a composite image (Nihei, et al., 2001).

Use of the finite-difference modeling technique is being extended to 3D, allowing investigation of azimuthally dependent scattering.

Conclusions

1) A realistic scale numerical model shows that energy scattered from discrete fractures or joints can be detected as coherent events in surface seismic data.
2) Fracture tip diffractions and P-to-S conversions appear to be the dominant events.
3) The stiffness of the fractures is a crucial parameter for detectability, while spatial scale and spacing are also important. We find that the range of stiffness deduced from our conceptual model should be detectable in field data.
4) Standard CMP processing will not correctly image these events, instead they will be attenuated because of non-hyperbolic moveout. We are investigating imaging methods using P-to-S conversions.

References

Coates, R. T., and Schoenberg, M., Finite-difference modeling of faults and fractures, Geophysics, **60**, n5, 1995.

Majer, E.L., T.M. Daley, L.R. Myer, K. Nihei, J. Queen, J. Sinton, J. Murphy, M. Fortuna, H.B. Lynn, M.A. Imhoff, R. Wilson, San Juan Fracture Characterization Project: Status and Current Results, LBNL-48908, Lawrence Berkeley National Laboratory Report, 2001.

Myer, L.R., Fractures as collections of cracks, International Journal of Rock Mechanics and Mining Sciences, **37**, p231, 2000.

Nihei, K.T., S. Nakagawa and L.R. Myer, Fracture imaging with converted elastic waves, Proc. of the US Rock Mech. Symp., Washington D.C., 2001.

Acknowledgments

This work was supported by the assistant Secretary for Fossil Energy, National Energy Technology Laboratory (NETL). LBNL processing was performed at the Center for Computational Seismology, supported by the Director, Office of Science, Office of Basic Energy Sciences, Division of Engineering and Geosciences, of the U.S. Department of Energy under Contract No. DE-AC03-76SF00098. We would like to thank NETL project managers Thomas Mroz and Frances Toro for their support.